

# Analysis of the “Mesh-Plane” HSI Image

*Terrance J. Gaetz*

In this chapter the analysis of the HSI “Mesh-plane” HSI images is considered.

## 21.1 Mesh-Plane HSI Image

It was noted from the time of the initial out-of-focus “first light” HSI images that such images might contain structure which could be used to assess the HRMA alignment. A number of out of focus exposures were made to study different aspects of the HRMA, most notably the ring focus tests (see Chapter 18). In addition, exposures were taken at what was then thought to be the mesh plane for the FPC detectors. The mesh plane was taken to be 9.7 mm behind the aperture plate, so that when the focus is at the aperture plane, the mesh plane would be 9.7 mm out of focus. Subsequent measurements indicate that the actual spacing between the mesh plane and the aperture plane was  $9.12 \pm 0.15$  mm. The “mesh plane” HSI exposures were requested at 9.7 mm out of focus, and the defocus value derived from the stage logs is consistent with 9.7 mm. It should also be noted that there may be some uncertainty in the relative axial location of the HSI relative to the FPC aperture plane; the value was originally measured before the HSI MCP failed and was replaced.

The images are too far from the finite conjugate focus to be of much help in assessing the shell-to-shell alignment, but are of great interest for assessing the effects of epoxy-induced distortion of the optic; the ring focus images are analyzed in detail in Chapter 18.

The “mesh plane” exposures turn out to provide useful alignment information and may also yield information on mirror deformations. Two mesh plane HSI exposures were taken, `hsi107550` and `hsi111803i0` (see Table 21.1). One image, `hsi111803i0`, is deep enough to provide useful information for assessing mirror shape and refining the HRMA alignment parameters; in this chapter, the analysis will concentrate on the `hsi111803i0` exposure.

The `hsi111803i0` image was taken at 9.7 mm aft of the focal plane. The image is far enough out of focus so that the rings from the individual shells are almost separated, but near enough to focus that the asymmetries and image deformations can be picked out. As such, this image will be important both for refining the alignment estimates, and for improving our understanding of the 1G mirror structural models.

The degapped HSI images `hsi107550` and `hsi111803i0` are shown in Figure 21.1. These image shows a number of interesting features, including:

Table 21.1: Mesh Plane HSI images

Date	TRW Test ID	runid	energy (keV)	exposure time (sec)	valid events
04 Jan 1997	D-IXH-PI-3.003	107550	1.49	104.002556	52073
10 Feb 1997	E-IXH-RF-18.002	111803	1.49	1032.847290	607305

- a distinctive braiding resulting from the 1G-induced distortions
- an enhanced central spot where the in-plane scattering planes intersect (visible in the hsi11803i0 image).
- the spoke shadows do not line up across the image; rather they are radial with respect to the enhanced central spot. Close inspection reveals offsets in the strut shadows between different shells; this is maybe most noticeable at the bottom of the image in comparing shell 4 to shell 6.
- mirror pair six (the smallest ring) is displaced down and somewhat to the left relative to the other rings.
- the larger rings show small displacements relative to each other.

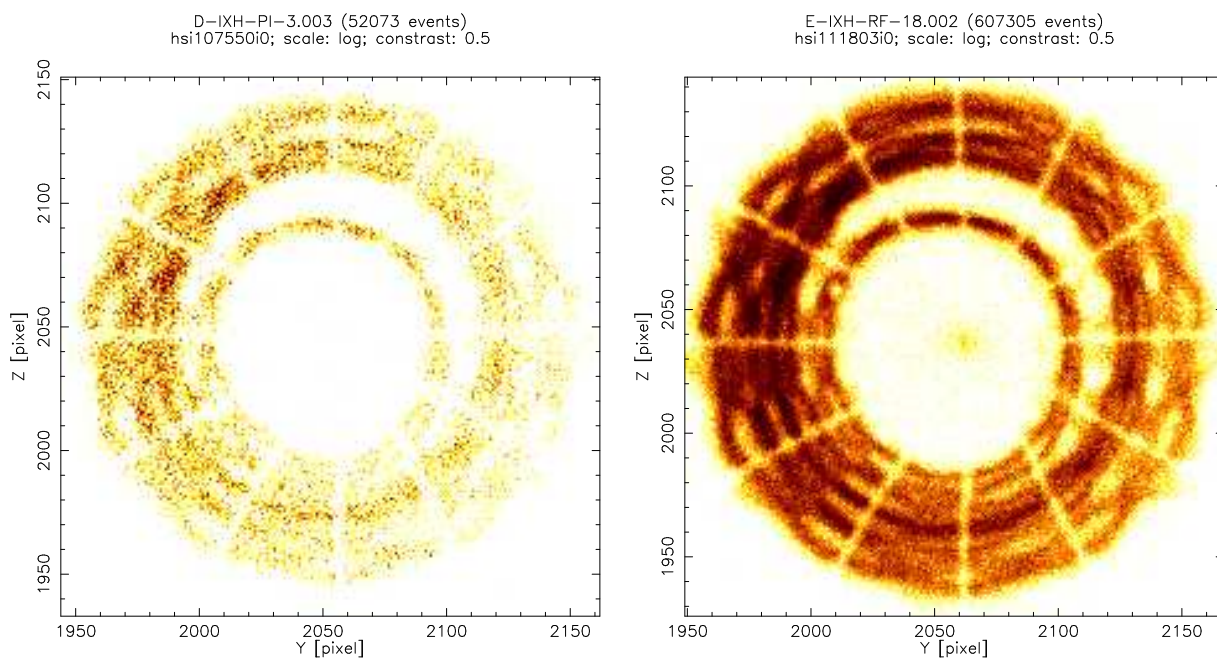


Figure 21.1: The two “mesh plane” HSI images. Left: hsi107550i0 image, stretch=log. Right: hsi111803i0 image, stretch=log.

## 21.2 Raytrace Simulations

To learn more about the implications of this image we turn to high fidelity raytrace models based on the SAO and the EKC finite element mechanical models for the distortion of the mirrors when supported horizontally under a 1G load. In the raytrace, the EIPS source distance was taken to be 527522 mm from the HRMA node, which is 18 mm from the P side of the CAP. Consequently, the source distance from the CAP DATUM –A– plane is 527504 mm.

Table 21.2: Focus distance from CAP Datum –A– plane for EIPS Al-K $\alpha$  source

1G model	Focus (mm)
SAO 1G model	10274.777
EKC 1G model	10274.691

Table 21.3: Vertical/Horizontal ratios for meshplane HSI image

Mirror Pair	HSI image	raytrace
1	0.99	0.95
6	1.08	1.02

Focus at Al-K $\alpha$  was determined by raytraces with ray density  $6 \text{ mm}^{-2}$  resulting in the values given in Table 21.2

Figure 21.2 compares the raytraced images based on the SAO and the EKC mechanical models with the `hsi111803i0` image; for reference, a raytrace with no 1G distortions is included. All three raytraces are based on the rigid body alignment model (EKCHDOS06) described in Jerius (1997).

Several things can be discerned by comparing these images:

- The overall scale of the HSI image appears to be slightly larger than the raytrace models. This suggests that the axial location for the ray projection may not be quite right.
- The shell 6 ring appears to be displaced downwards more in the HSI image than in the raytraces. This suggests that the rigid body “tilt” parameters may be slightly off.
- Close examination of the XRCF image shows that the innermost and outermost shells are relatively cleanly visible; the middle two mirror pairs are somewhat more confused and care is needed in interpreting the image. It may be possible to slice out rings 1 and 6 from the HSI image; rings 3 and 4 are too close together and overlap in places.
- The ratio of the vertical to horizontal dimensions differs somewhat between the XRCF image and the raytrace simulations. Crude estimates of the vertical to horizontal ratios for the SAO 1G model are compared to the estimates for the HSI image in Table 21.3. This suggests that the mechanical models predict somewhat more ovalization than is seen in the XRCF data.
- The shape of the shell 6 ring is slightly different than in the raytrace model.

We address these issues in the following sections.

## 21.3 Analysis of the Image

In order to assess the HSI image, the image was clipped into three quasi-elliptical annuli covering mainly shell 6, shells 3 plus 4, and mainly shell 1. Each annulus was bounded by an ellipse. The annuli used for the HSI image are given in Table 21.4; these cuts are plotted in Figure 21.3. For comparison, Figure 21.4 shows raytrace simulations based on the SAO 1G model. **needed: similar figures for EKC model.**

The shell 1 and shell 6 rings were analyzed using the ring analysis software. The mean ring radius for the HSI rings as a function of azimuth is plotted in Figure 21.5. For comparison, the same analysis is presented for the SAO 1G model. **To be done: a similar treatment for the**

Table 21.4: Parameters for the quasi-elliptical annuli used to split apart the hsi111803i0 image

Mirror Pair	$a_i$	$a_i/b_i$	$Y_i$	$Z_i$	$a_o$	$a_o/b_o$	$Y_o$	$Z_o$
1	83	1.03	2057	2038	104	1.03	2037	2037
3+4	59	1.07	2055	2035	83	1.03	2057	2038
6	40	1.07	2055	2035	59	1.07	2055	2035

Table 21.5: Ring radius parameters.

Mirror Pair	$R_{hsi,avg}$ (HSI pixel)	$R_{raytrace,avg}$ (HSI pixel)	ratio	$\Delta F$ (mm)
1	93.22	87.41	1.066	0.640
6	52.44	47.45	1.105	1.020

**EKC 1G model. Also, Fourier analysis of the curve. Can we dig out ovalization and trefoil (to compare to the models)? Can we get a tilt estimator out of it?**

In Table 21.5 some parameters of the ring fits are presented. The  $R_{hsi,avg}$  column gives the mean radius for the rings in the HSI image, while  $R_{raytrace,avg}$  gives the values for the raytraces. The ratio column is  $R_{hsi,avg}/R_{raytrace,avg}$ . The  $\Delta F$  column lists the additional defocus distance needed to make the mean ring radius in the raytrace match the mean ring radius in the HSI image, assuming that defocus is the only effect operating. **The raytrace setup needs to be rechecked to make sure I haven't entered a distance incorrectly or something. If that doesn't explain it, we need some comment on this. How much can be plausibly attributed to the HSI position relative to the FPCs? How much is a result of mirror deformations (1G or other) biasing the radius estimator? My earlier estimates based on measuring the image with a ruler gave a defocus correction of about 0.4 mm compared to 0.64 and 1.02 here. ???**

### 21.3.1 Axial position of the image

Recent reexamination of the XRCF focus data indicates that the axial position of the HRMA is not repeatable at the level of

[http://hea-www.harvard.edu/MST/simul/xrcf/HRMA/focus/hsi\\_offset/index.html](http://hea-www.harvard.edu/MST/simul/xrcf/HRMA/focus/hsi_offset/index.html)

## 21.4 Updating the Tilts

As noted above, the displacement of the shell 6 ring relative to the others seems to be somewhat larger than in the raytrace models based on the EKCHDOS06 version of the rigid-body parameters. In the analysis of the mirror “tilts” based on the quadrant shutter focus studies (see Jerius (1997)) it was found that the “Y-tilts” were larger than predicted by the models. Based on comparison with the predictions of the EKC 1G model and the SAO 1G model, it was concluded that the discrepancy was likely a result of 1G tilts not captured by the modeling.

These additional Y-tilts are here applied to the raytrace model; the Y-tilt differences *only* from line E of Table 11.2 of Jerius (1997) were applied. In addition, a 0.1 " Z-tilt was applied to shell

6 only in order to improve agreement with the HSI image. These are relative P to H tilts for individual mirror pairs. In order to retain nearly the same parfocalization as before, the additional tilts were applied half to the P optics and half to the H optic of a given mirror pair, but with opposite signs.

**To get the overall scales to match, I had to project the raytrace an additional 0.4 mm or so; the stage logs indicate that the HSI image was taken at 9.7 mm back from the on-axis HRMA focus; the reason for this difference needs to be elucidated. The XRCF focus is calculated using quad-shutters while the raytrace focus is determined using saofocus with scattering turned off (minimizing rms blur); could the difference in focus algorithms be introducing an offset in where the focus appears to be?**

(Note added 980501: source distance error for the EIPS distance in the raytrace may account for 0.1 mm or so of the discrepancy.)

(Note added 980826: The source distance has been fixed, but not all the raytraces have been redone yet. The “ring focus” style analysis above indicates a larger than that I estimated here; what about the effects of mirror deformations?) Figure 21.6 compares the HSI image to the raytrace results with 0.5, 1, and 1.5 times the additional Y-tilts. Similarly, Figure 21.7, shows the effect of adding 0, 1, and 2 times the additional Z-tilt to a model to which the additional Y-tilts have already been added.

In Figure 21.8 the raytrace model (including the additional tilts based on the quadrant shutter data) is compared to the HSI image.

## 21.5 Mirror Distortions

based on Fourier Analysis above, or by empirically comparing raytrace models to the HSI image. Extract the 2nd & 3rd order DDR's from WAP's Assembly Strain .DFR files and compare.

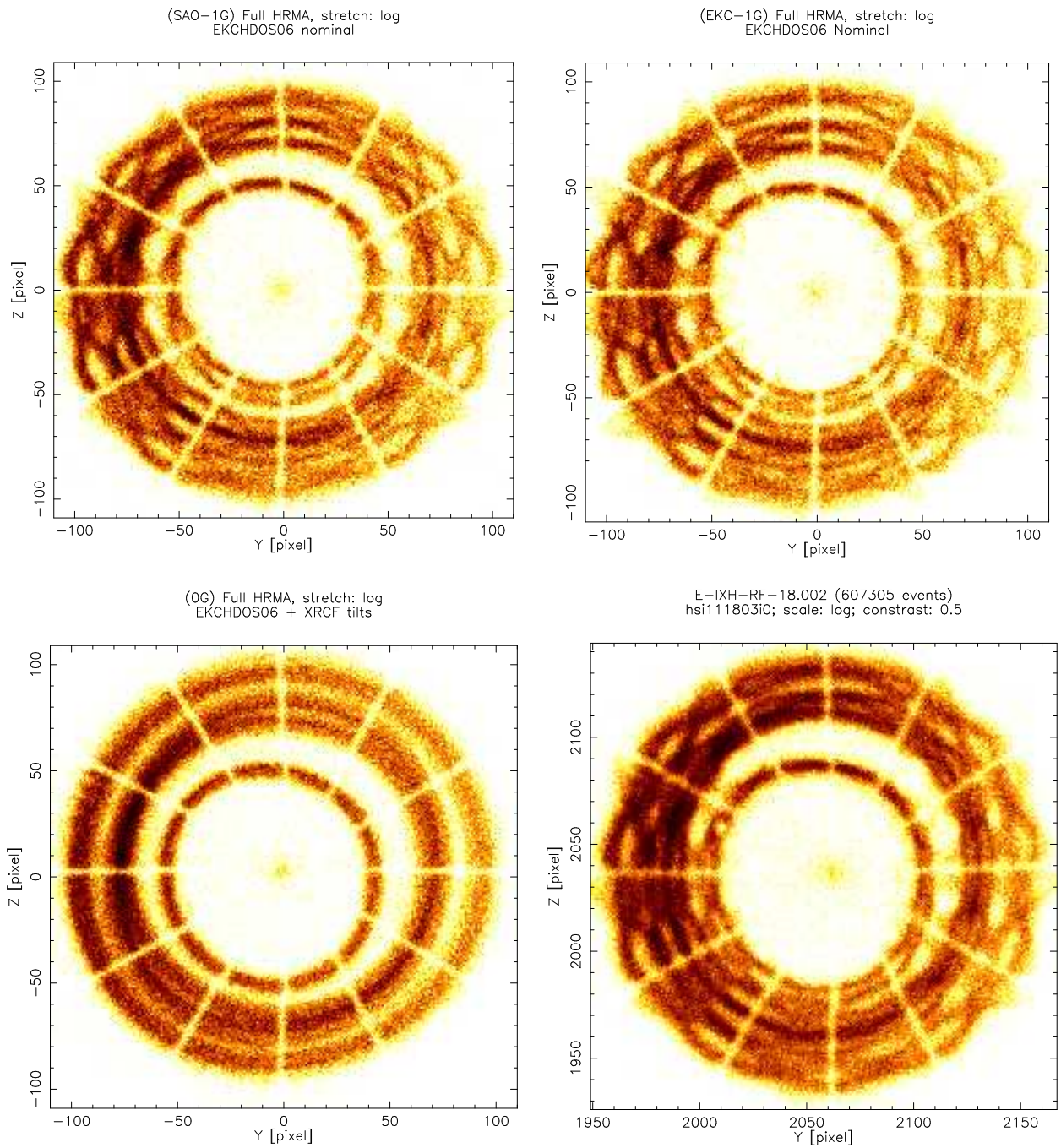


Figure 21.2: Raytrace simulation comparing the SAO and the EKC 1G mechanical models. These traces differ only in the 1G model used; all other components (alignment parameters, assembly strain terms, epoxy shrinkage) are the same. The rigid body alignment terms are those given in the MST Phase 1 preliminary report (EKCHDOS06 rigid body terms). Top Left: SAO 1G nominal case, EKCHDOS06 rigid body terms, log stretch. Top Right: EKC 1G nominal case, EKCHDOS06 rigid body terms, log stretch. Bottom Left: 0G case, EKCHDOS06 rigid body terms, XRCF tilt corrections, log stretch. Bottom Right: hsi111803i0 image, log stretch.

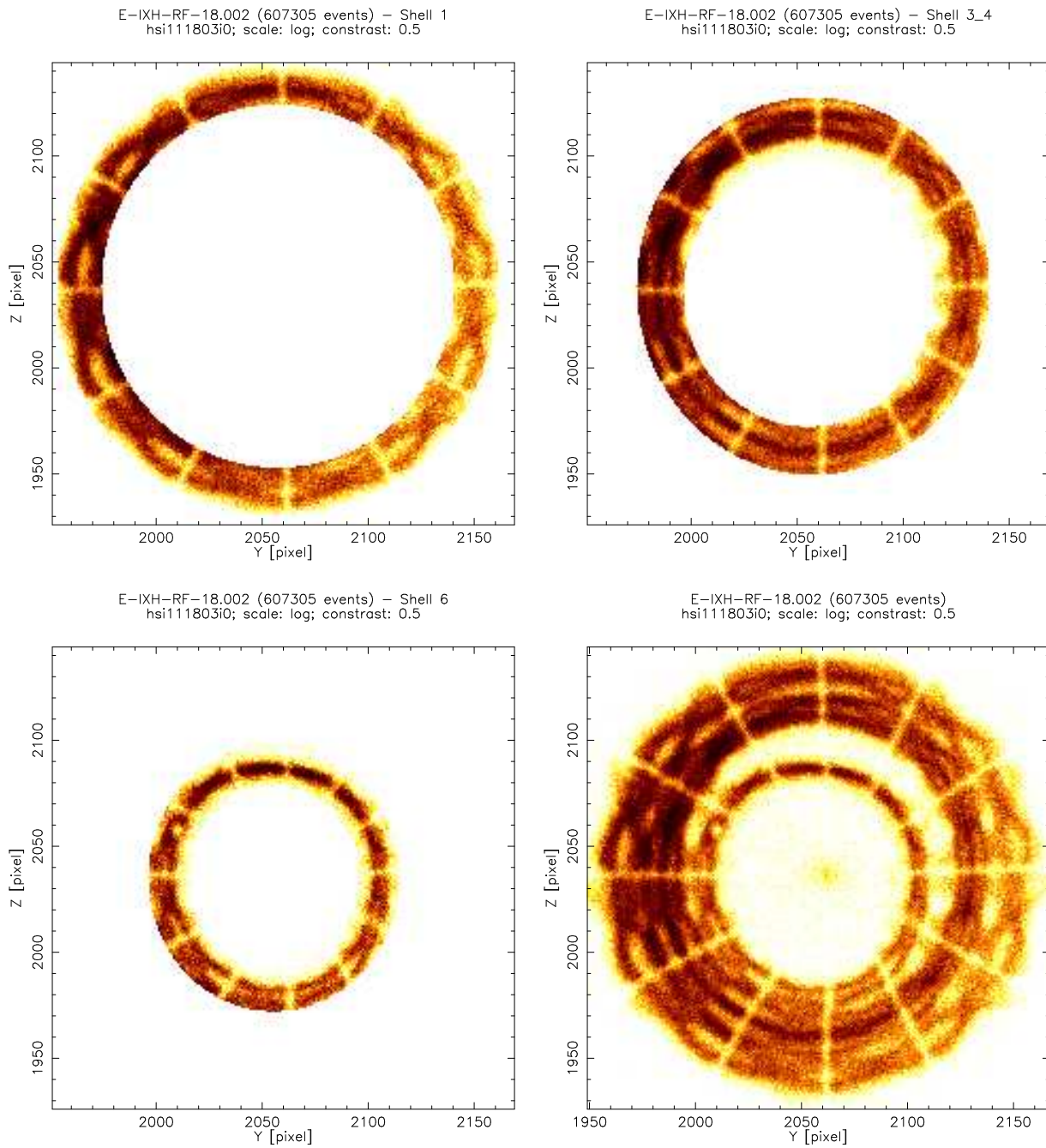


Figure 21.3: Division of hsi111803i0 image into annuli. Top left: shell 1, stretch=log. Top right: shell 3 + 4, stretch=log. Bottom left: shell 6, stretch=log. Bottom right: full hsi111803i0 image, stretch=log.

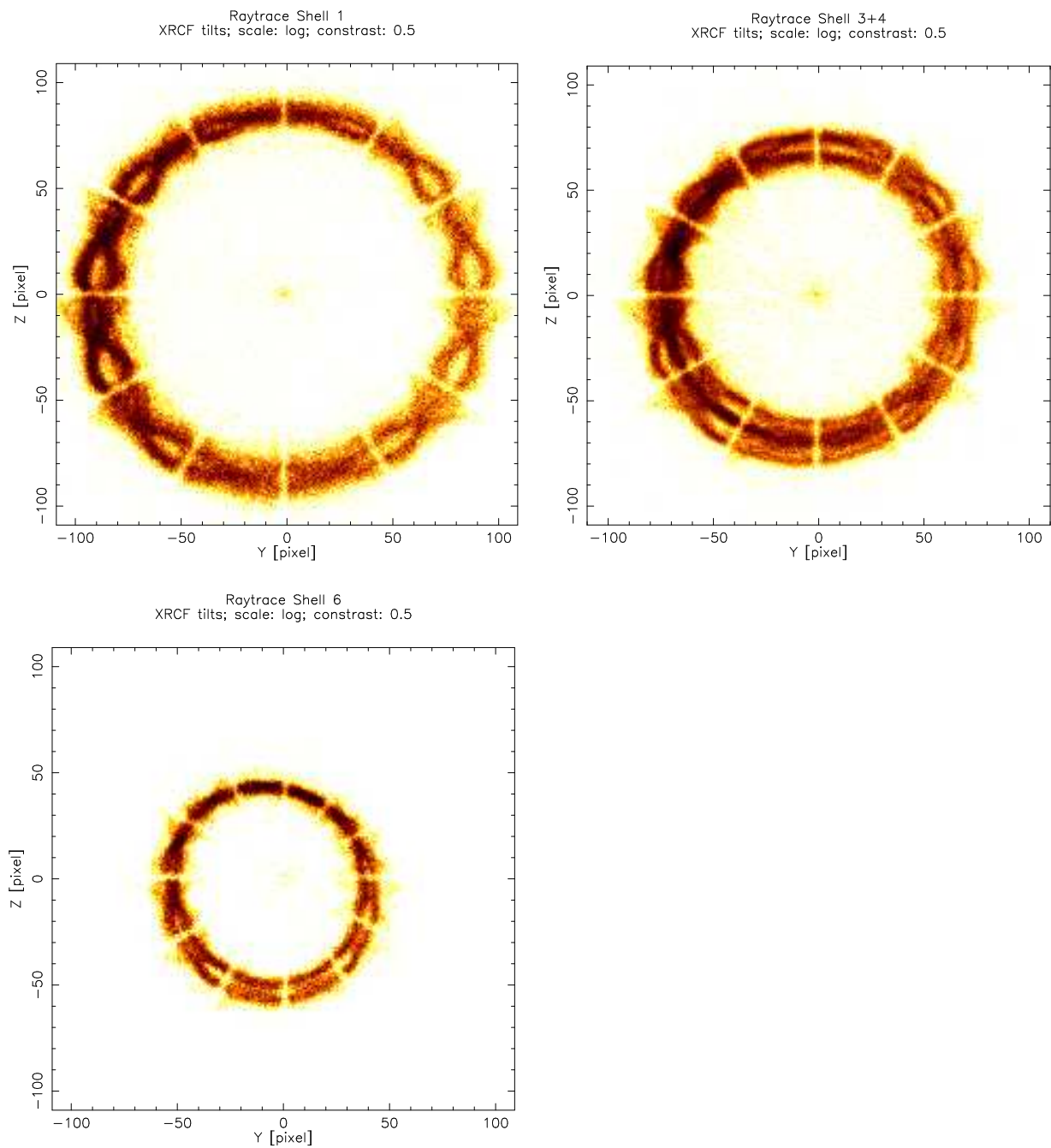


Figure 21.4: Raytraces for individual HRMA shells, or Mirror Pairs (MP), at the “mesh plane”. Top left: shell 1, stretch=log. Top right: shell 3 + 4, stretch=log. Bottom left: shell 6, stretch=log.



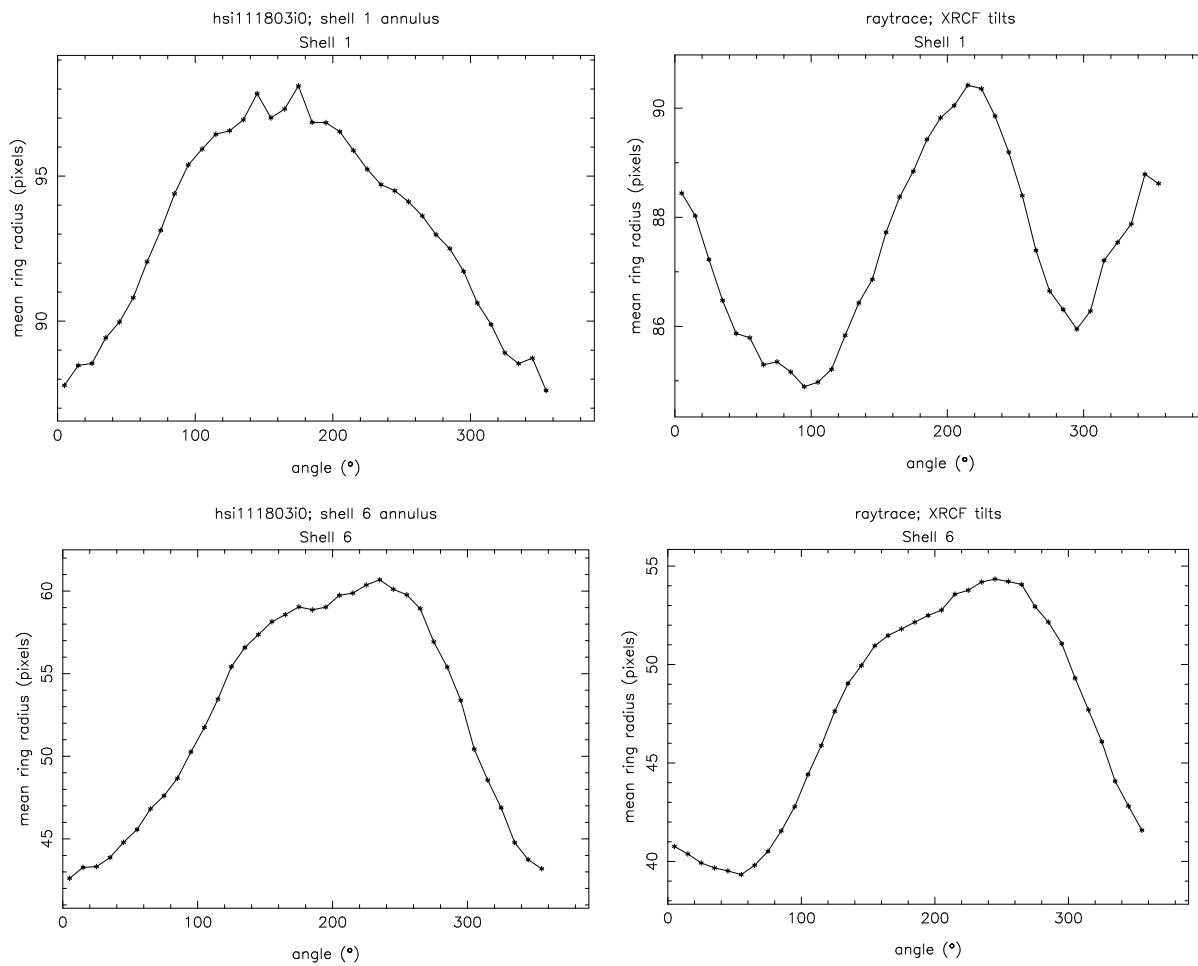


Figure 21.5: Ring radius for individual shells. Top left: shell 1, hsi111803i0 image. Top right: shell 1, raytrace. Bottom left: shell 6, hsi111803i0 image. Bottom right: shell 6, raytrace.

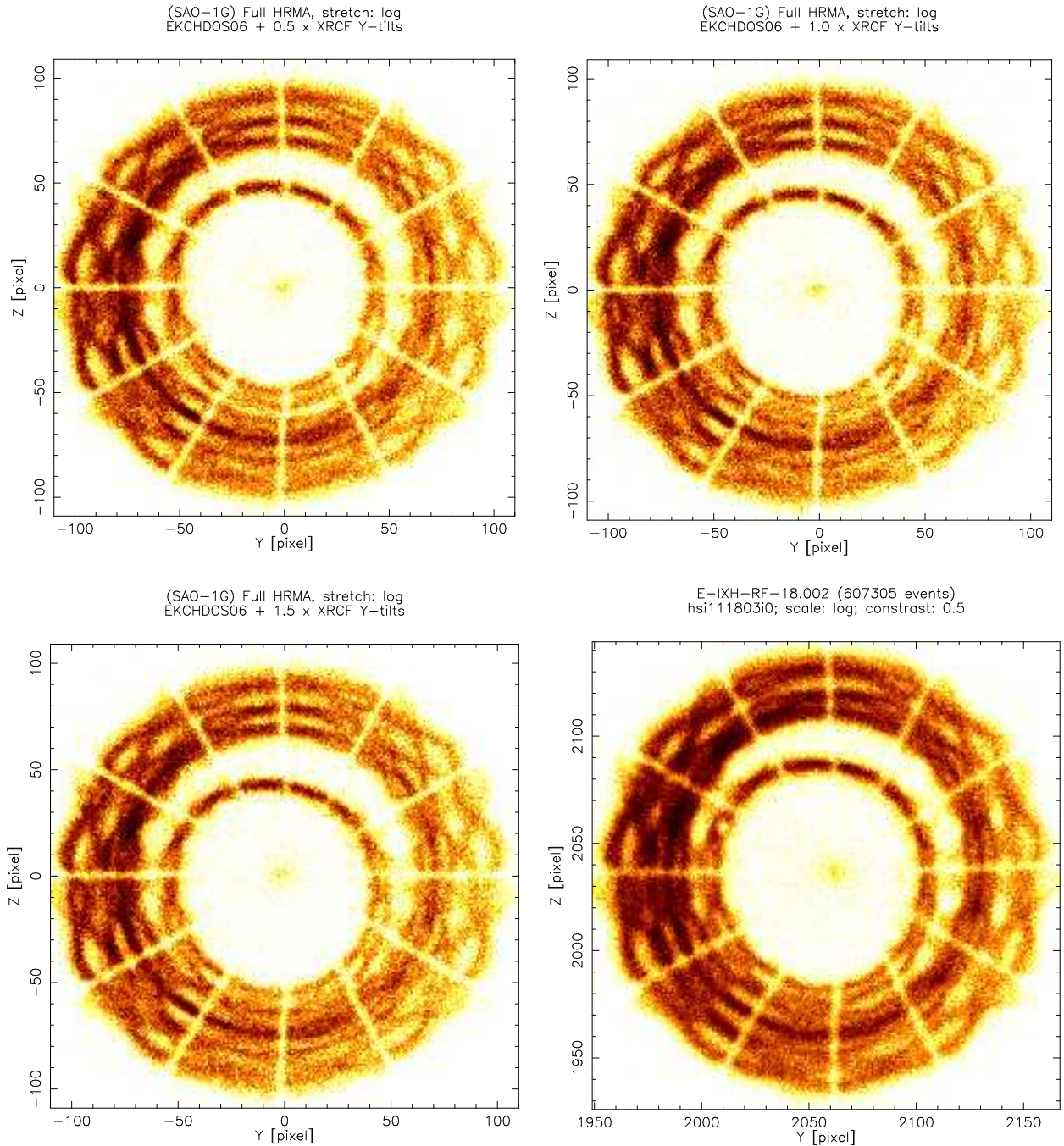


Figure 21.6: Raytraces with varying Y-tilts compared to hsi11803 image. Top left:  $0.5 \times \text{XRCF}$  Y-tilts, stretch=log. Top right:  $1.0 \times \text{XRCF}$  Y-tilts, stretch=log. Bottom left:  $1.5 \times \text{XRCF}$  Y-tilts, stretch=log. Top right: hsi11803i0 image, stretch=log. The images are sqrt stretched.

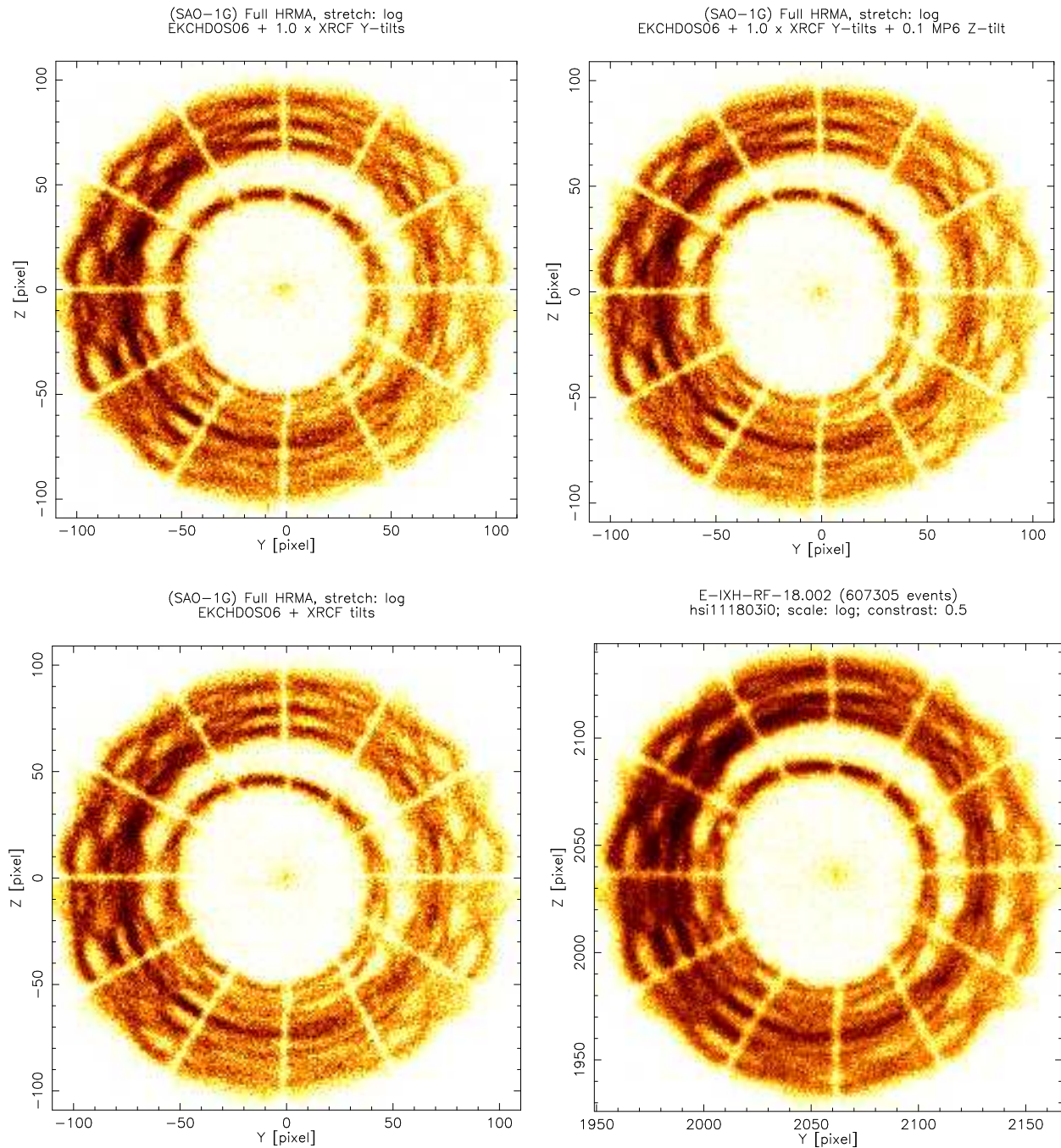


Figure 21.7: Raytraces with varying Z-tilts compared to hsi11803 image. Top left: XRCF Y-tilts;  $0.0''$  added P6 Z-tilt, stretch=log. Top right: XRCF Y-tilts;  $0.2''$  added P6 Z-tilt, stretch=log. Bottom left: XRCF Y-tilts;  $0.1''$  added P6 Z-tilt, stretch=log. Top right: hsi111803i0 image, stretch=log.

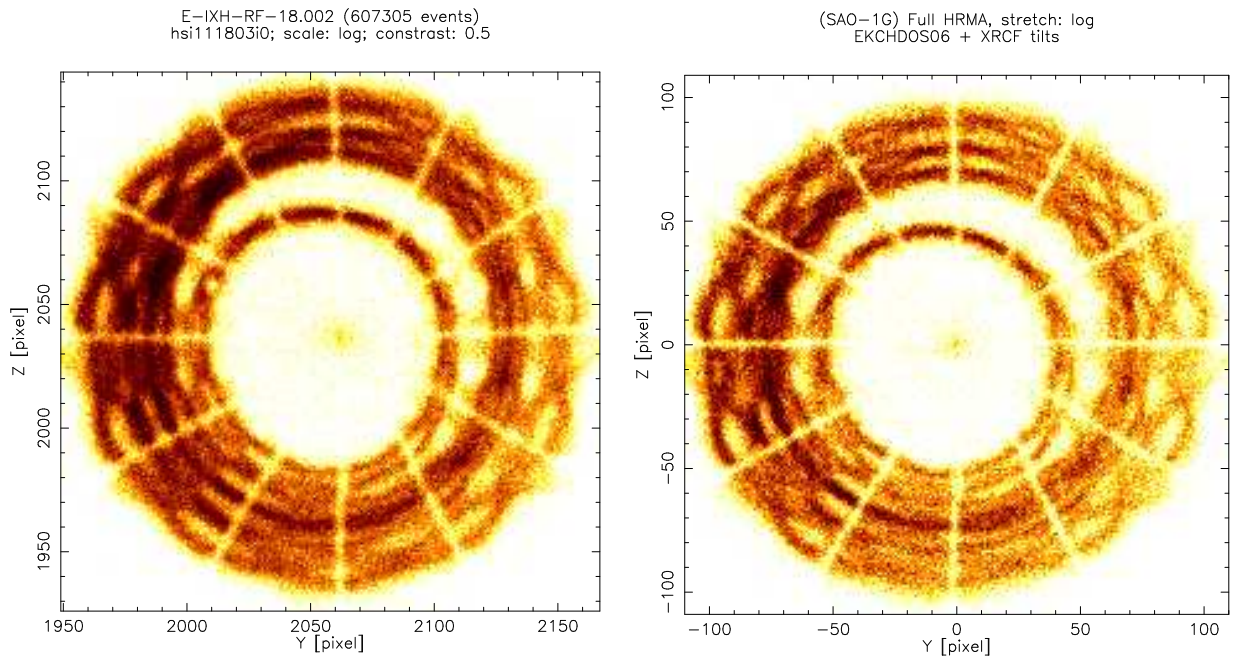


Figure 21.8: Comparison of XRCF mesh plane HSI image (top) and raytrace simulations (bottom). Left: hsi111803i0 image, linear stretch. Right: HRMA raytrace, SAO-1G model, EKCHDOS06 rigid body terms, XRCF tilt correction, log stretch.